Palaeogeography, Palaeoclimatology, Palaeoecology 574 (2021) 110475

Contents lists available at ScienceDirect

Palaeogeography, Palaeoclimatology, Palaeoecology

journal homepage: www.elsevier.com/locate/palaeo

Invited Research Article

A multi-proxy reconstruction of the late Holocene climate evolution in the Kapsabet Swamp, Kenya (East Africa)

Dennis M. Njagi [a,b], Joyanto Routh [a,*], Daniel Olago [b], Kasun Gayantha [c]

[a] Department of Thematic Study - Environmental Change, Linköping University, 58183 Linköping, Sweden
[b] Department of Geology, University of Nairobi, PO Box 30197-00100, Nairobi, Kenya
[c] Max Planck Institute for Biogeochemistry, 07745 Jena, Germany

ARTICLE INFO

Editor: Dr Shucheng Xie

Keywords:
Highland peat
Carbon
Stable isotopes
Biomarkers
Paleoclimate

ABSTRACT

Multi-proxy high-resolution records relating to climate and dominant vegetation cover have been obtained from a peat deposit retrieved from the Kapsabet swamp in western Kenya. The 4-m long peat sequence provided a continuous sedimentation record spanning ca. 3023 cal yr BP to the present and is representative of the late Holocene changes in the relatively high-altitude part of the Lake Victoria catchment. Paleoenvironmental factors influencing peat formation and organic matter (OM) source inputs in Kapsabet were reconstructed based on total organic carbon, carbon accumulation rate, $\delta^{13}C$, $\delta^{15}N$, C/N ratio, and specific biomarker-based *n*-alkane ratios. The Kapsabet peat sequence was divided into five stages based on different climatic conditions: Stage 1 (3023–1670 cal yr BP) represents a progression from cool dry to wet conditions. Stage 2 (1670–1187 cal yr BP) is a relatively warm and wet period with increased productivity and high OM input. Stage 3 (1187–625 cal yr BP) represents gradual warming coeval to the late Holocene Medieval Warm Period. Stage 4 (625–188 cal yr BP) is a cool and wet period with high variability in precipitation and hydrological conditions representing the Little Ice Age. Stage 5 (188 cal yr BP to present) represents a relatively cool and wet period that coincides with the expansion of agriculture, particularly in the lowlands. The proxies indicate a progressive change from a forested landscape to an open woodland coeval to a decline in terrigenous inputs and the advent of more wet conditions. The climate on the highlands was less variable than in the lowlands, which underwent several periods of drought and intermittent wet conditions. The changes in the catchment coincided with the expansion of agriculture and land clearance marking increased human activities in the lowlands. Overall, the Kapsabet peat sequence tracks the regional climatic changes in East Africa and marks a promising sedimentary archive for palaeoclimate reconstruction from a region with a paucity of palaeoenvironmental and palaeovegetation histories.

1. Introduction

The climate in East Africa has undergone substantial decadal- to millennial-scale changes during the Holocene, first driven by natural processes, and later, by humans, as pastoral lifestyles gave way to sedentary and then urbanised communities (Kiage and Liu, 2006; Marchant et al., 2018; Chritz et al., 2019). The natural processes included rapid changes in hydrological conditions during the mid- to late Holocene, a period which has been related to the changing position of the Intertropical Convergence Zone (ITCZ) and local to regional feedbacks associated with the variations in small to large lake systems, vegetation cover, soil characteristics, and topography over differing time scales (Tiercelin and Lezzar, 2002; Kiage and Liu, 2006; Olago et al., 2009; Olaka et al., 2010; Trauth et al., 2010; WoldeGabriel et al., 2016; Marchant et al., 2018). The palaeoecological, palaeoclimatological, and palaeohydrological evidence cited by these and other authors indicate that precipitation regimes can change quickly (over decades), and they are not necessarily always synchronous over large swathes of the region. These studies have mainly focused on lacustrine and occasionally peat sequences to trace the environmental perturbations, ecological shifts and human-environment interactions that have been highly responsive to local and regional changes in natural climatic perturbations, hydrology and anthropogenic disturbances (Russell et al., 2007; Strack, 2008; Marchant et al., 2018; Opiyo et al., 2019). Paleoenvironmental inferences from multi-proxy data suggest the prevalence of variable (wet to dry conditions) at about 4000 cal yr

* Corresponding author.
E-mail address: joyanto.routh@liu.se (J. Routh).

https://doi.org/10.1016/j.palaeo.2021.110475
Received 23 September 2020; Received in revised form 8 May 2021; Accepted 12 May 2021
Available online 15 May 2021

BP in the wider East African region (Russell and Johnson, 2005; Marchant et al., 2018 and references therein) and in the Lake Victoria basin (Talbot and Lærdal, 2000; Stager et al., 2005; Berke et al., 2012). However, in the vast Lake Victoria basin with a catchment area of 184,000 km^2, the climatic and environmental changes during this period are spatially and temporally poorly resolved, especially in the highlands.

It is noted that the formation of peat deposits in western East Africa is related to increased moisture, temperature, and waterlogging effects (Marchant et al., 2018). The peat deposits developed in semi-arid regions along an altitudinal sequence forming a string of promising climate archives (see Kiage and Liu, 2006; Marchant et al., 2018). Peat accumulation at a higher elevation, such as the Kuwasenkoko or Muchoya Swamps, was less (2340 and 2260 m asl, respectively; Hamilton, 1982) compared to swamps at lower elevations, including the Ahakagyezi Swamp (1830 m asl) in Uganda (Taylor, 1990). However, local terrain plays an important role in peat formation and the highland Kapkanyar Swamp in the Cherangani Hills (2422 m asl) in Kenya reaches a depth of 3.5 m (Opiyo et al., 2019). The ability of peat to accumulate rapidly (0.5–1.0 mm yr^{-1}; Parish et al., 2008) and preserve detailed palaeoenvironmental records make these deposits extremely suitable for Holocene studies (Chambers and Charman, 2004; Zheng et al., 2007; Routh et al., 2014; Payne et al., 2015; Baker et al., 2014, 2016). Therefore, in the tropics, peatlands serve as an alternative to ice cores and ocean sediments due to their accessibility and cost-effectiveness in retrieving promising sediment cores for high-resolution paleoclimate reconstruction (Chambers and Charman, 2004). Marchant et al. (2018) note the presence of a number of these organic-rich mires and peat deposits in East Africa and that they have not been described in detail or investigated for climate studies. Some older low-resolution records such as the Labot and Loboi swamps in Kenya (Hamilton, 1982; Ashley et al., 2004) and Ahakagyezi and Muchoya swamps in Uganda (Taylor, 1990) provide information about paleoclimatic conditions based on vegetation (pollen assemblages) and sedimentology since the late Pleistocene. However, these studies provide limited information about changes since the mid-to-late Holocene epoch.

The Intergovernmental Panel on Climate Change cites the poor record of proxy-based climate reconstruction from Africa due to the limited number of high-resolution records used for predictive models for regional climate assessment (Niang et al., 2014). Hence this study focuses on reconstructing a high-resolution record of paleoenvironmental conditions in the Kapsabet Swamp located in the eastern highland portion of the Lake Victoria catchment in western Kenya. These mires have developed because of incomplete decomposition of organic matter, fresh litter input from vegetation, water-logging, and anoxic conditions. The main source of water is from rainfall (ombrotrophic conditions), with relief supporting water-logging and peat formation. The actively forming peat deposit reaches a depth of 4 m (or possibly more). Multiple geochemical proxy signatures, including the organic matter (OM) characteristics such as total organic carbon (TOC), total nitrogen (TN), C/N, bulk $\delta^{13}C$, bulk $\delta^{15}N$ and *n*-alkane biomarker ratios were investigated. The diagnostic biomarker ratios included terrestrial/aquatic ratio (TAR), aquatic plant index (P_{aq}), carbon preference index (CPI) and average chain length (ACL) that were used to reconstruct the palaeoenvironmental and palaeoclimatic conditions in the eastern highlands of Lake Victoria during the past 3000 years. To the best of our knowledge, this is the second record of a highland peat sequence from the Lake Victoria basin covering the palaeoenvironmental changes in East Africa since the late Holocene after Opiyo et al. (2019). Opiyo and co-authors used radiocarbon dates covering the period 3000 yr BP to present, representing a similar time interval to the Kapsabet core. Consequently, comparisons between these areas and information from previous studies, as mentioned earlier, provide an opportunity to discern the spatio-temporal climate-environment changes in this region.

2. Materials and methods

2.1. Study area

The sampling site is about 400 km from Nairobi, Kenya, on the western part of the Rift Valley. It is located in Kapsabet County and is part of the Kingwal Swamp, a wetland in the upper catchment of River Yala (Raburu, 2005). As a typical wetland (Keddy, 2010), the swamp exhibits characteristics of both terrestrial and aquatic ecosystems and is driven by biotic and abiotic processes from inundation by water. Rainfall in the area ranges between 1200 and 2000 mm/year. The long and more intense rainy season extends from March to June, whereas the short period extends from September to November. The mean annual temperature range is 16 °C to 22 °C (Songok et al., 2011).

The regional geology is made up mostly of volcanic rocks. In the rolling hills in the west of the study area, pelitic gneisses, migmatites and granites make up the basement. The Uasin Gishu plateau in the northeast is made up of phonolites. The Tinderet Highlands in the south consists of tuff and agglomerate flows that underlie the swamp (Jennings, 1964). Drainage in the area is structurally and geologically controlled. The wetland is partially fed by the Kesses River from the east and drained by Kingwal River in the west (Sitienei et al., 2012). The Kingwal and Kiterges Rivers and their tributaries drain into the northwestern flank of Tinderet Highlands. The rivers running over the Uasin Gishu plateau form a sub-parallel drainage pattern that cuts the lava surface and flows northwest. Rivers in the Tinderet Highlands exhibit a radial drainage pattern except for the Kipkurere and Meteitei Rivers that flow southwest. The Kimondi and Mokong River systems descend the Nyando escarpment and face in a parallel pattern to join River Yala (Jennings, 1964).

Achieng' et al. (2014) found that there are about 110 plant species in 39 families in the Kingwal Swamp which were categorized into aquatic (35), semi-aquatic (17) and terrestrial (59) species. Vegetation types in the swamp were divided into four dominant zones consisting of semi-aquatic plants, *Floscopa, Pycreus* and *Cyperus* spp. The wetland was also represented by moderately abundant vascular plants, algae, and sedges. Vegetation types in the neighbouring area include forests, grasslands and shrublands. The forest cover includes about 70 species from 37 different families and 60 genera of woody and non-woody plants, with *Euphorbiaceae, Rubiaceae, Rutacea, Bignoniaceae*, *Meliaceae*, *Moraceae* and *Ulmaceae* families being dominant (c. 50%; Maua et al., 2020). Dominant tree types include *Polyscias fulva*, *Tabernaemontana stapfiana*, *Ficus sur* and *Croton megalocarpus*. Other common species include *Solanum mauritianum*, *Syzygium guineense, Lepidotrichilia volkensii* and *Dombeya torrida (*Maua et al., 2020). Dominant grass species include *Andropogon gayanus, Heteropogon contortus, Panicum maximum* and *Sporobolus pyramidalis,* which are C4 type graminoids. About 40% of the swamp area has been converted into *Eucalyptus*, neem and teak plantations as part of the forest management initiatives (Sitienei et al., 2012). The wetland also offers a habitat for crested cranes, swamp deer and other animals (Sitienei et al., 2012). Population around the wetland is around 20,000 people, and major occupations are brickmaking, grazing and cultivation of maize and vegetables (Momanyi and Ariya, 2015).

2.2. Sampling

A core was recovered from a peat deposit near Kapsabet during a field expedition in August 2014 (Fig. 1). Core KP1A (0°05′26.0″N 35°09′07.0″E; 1863 ± 3.4 m a.s.l.) was recovered using a Russian peat borer (5-cm diameter x 50-cm length). The continuous undisturbed core extended to a depth of 4-m. The core was photographed, logged, and described in the field. Two other parallel cores were collected from the site within a 5-m distance. The cores were packed and transported in half-meter-long PVC pipes and stored at −18 °C once they reached Sweden. The KP1A core was sub-sampled at 1-cm intervals and freeze-

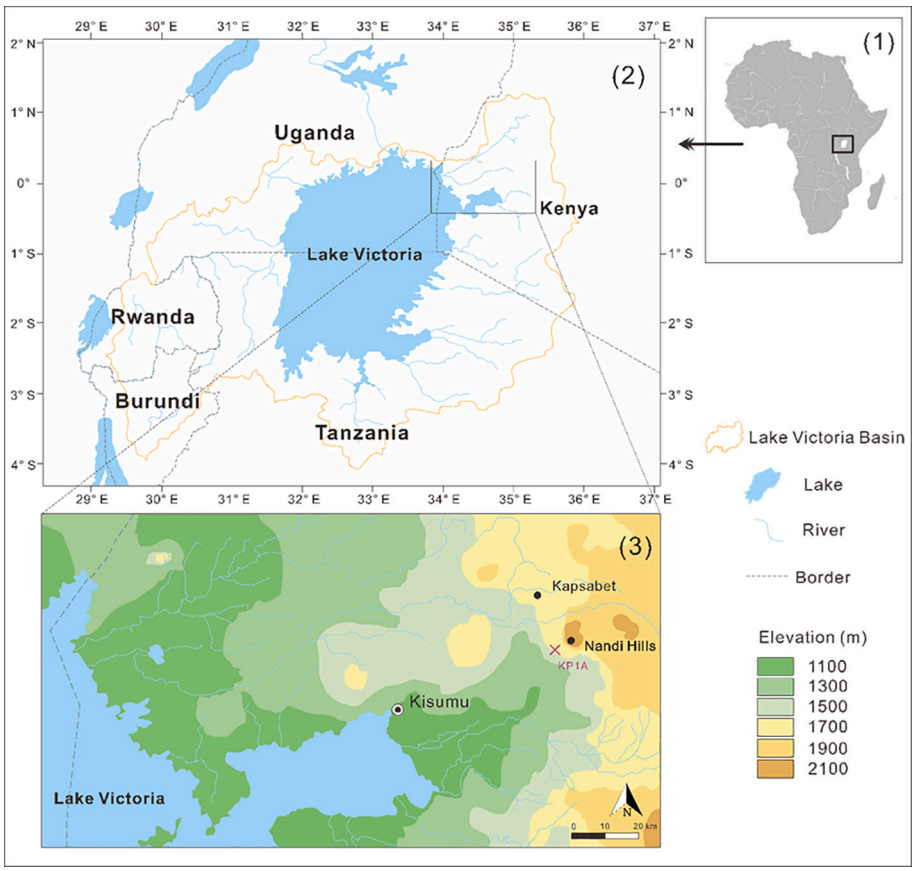

Fig. 1. Location of the sampling site in the Kapsabet peat deposit (KP1A) from western Kenya. (1) Lake Victoria and East Africa, (2) Lake Victoria catchment, and (3) Kapsabet swamp KP1A site.

dried. Weights were taken before and after drying to calculate the bulk density and porosity.

2.3. Radiocarbon dating

Radiocarbon dating was done on samples from 8 depth intervals in the KP1A core. Rootlets and other plant fragments were removed from samples, and the bulk samples were submitted for ^{14}C dating at the Poznan Radiocarbon Laboratory in Poland. The sediments were chemically pre-treated, as described by Brock et al. (2010). The method involved removing plant matter from the samples by sieving and manual extraction, followed by the acid-base-acid treatment (treatment with 1 M HCl or1M NaOH was followed by rinsing in ultrapure water). The product was centrifuged to remove excess liquid before it was freeze-dried. Finally, the samples were combusted with CuO and Ag wool at 900 °C for 10 h, and the CO_2 was reduced to pure graphite in a vacuum line as described by Czernik and Goslar (2001). Coal or IAEA C1 Carrara Marble and international modern Oxalic Acid II standards were subjected to the same pretreatment and combustion procedures. The ^{14}C content of the samples was measured using Compact Carbon Accelerator Mass Spectrometry (AMS) as per Goslar et al. (2004). The conventional ^{14}C age was calculated using a correction factor for isotopic fractionation described by Stuiver and Polach (1977).

Dates were calibrated using the Northern Hemisphere terrestrial calibration curve IntCal20 (Reimer et al., 2006) and using the Clam R software package (Blaauw, 2010). All ages were treated within a Bayesian framework using BACON – an R software package for age-depth modelling (Blaauw and Christeny, 2011). BACON divides a core into vertical sections and uses Markov Chain Monte Carlo (MCMC) iterations to estimate the accumulation rate (in years/cm) for each of the sections. Combined with the estimated starting date for the first section, the accumulation rate in each section was generated together to form the age-depth model (Blaauw and Christeny, 2011). In the age-depth model for KP1A core (Fig. 2), accumulation rates were constrained by a gamma distribution with a mean of 10 yr/cm. The age model was extrapolated to 0 cm (minimum depth) and 400 cm (maximum depth), assuming the core top (0 cm) represents modern age (−60 cal yr BP/ 2010 CE) to achieve the respective ages for each layer in the whole core.

2.4. Analytical procedures for paleoclimate proxies

Ninety-nine freeze-dried samples weighing 500 mg each were extracted at 8-cm intervals for C (organic), N (total), $\delta^{13}C$ and $\delta^{15}N$ analyses. The analysis was done at the Stable Isotope Geoscience Facility at Texas A&M University, USA. The samples were combusted (at 1020 °C) in an elemental analyzer (Carlo Erba NA 1500 Series 2) linked to an isotope ratio mass spectrometer (Thermo Finnigan Delta Plus XP). The C isotope composition was reported relative to the Vienna Pee Dee Belemnite (V-PDB) standard, whereas the N isotope composition was expressed relative to atmospheric nitrogen. Quality control was assured by running external standards, namely, Jet Rock 1 (NGS-JR-1) and Svalbard Rock 1 (NGS-SR-1). The analytical precision based on replicate analyses of standards were C ± 0.04% and ± 0.05‰ and N ± 0.006% and 0.08‰, respectively.

A total of 48 samples representing different lithologies were selected from the core and extracted for lipids using a modified protocol proposed by Wakeham et al. (2002). The extracts were analysed for *n*-alkane concentrations. Approximately 2 g of freeze-dried sediment was extracted with a spike of 50 mg/l *n*-hexatriacontane-d50 as a recovery standard. The extraction was done with a mixture of dichloromethane and methanol (9:1) on a Dionex ASE 300 Automated Solvent Extractor (3 cycles; 1500 psi at 100 °C). The total lipid extract (TLE) was

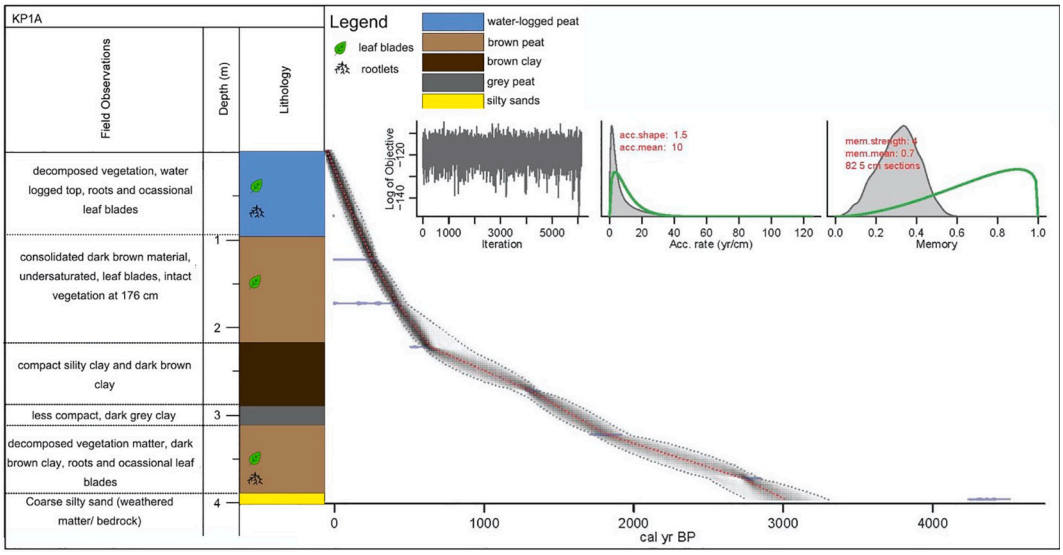

Fig. 2. Age-depth model and lithology for the Kapsabet peat deposit. The calibrated ^{14}C dates (transparent blue) and the age-depth model (darker grey indicates calendar ages; grey stippled lines show 95% confidence intervals). (For interpretation of the references to colour in this figure legend, the reader is referred to the web version of this article.)

evaporated under reduced pressure using a Buchi Syncore attached to a Buchi v-700 vacuum pump and reduced to dryness under nitrogen and then re-dissolved in a mixture of dichloromethane and isopropanol (2:1). The sample was separated using the solid phase extraction technique (SPE) to separate the fatty acids and neutral lipid fractions from the TLE using aminopropyl LC-NH_2 cartridges. The neutral fraction was eluted with 15 ml of a dichloromethane-isopropanol mixture (2:1), reduced under pressure, and taken to dryness under nitrogen.

The neutral fraction was eluted into alkanes and sterols using the cyanopropyl-silica bilayer cartridges. Alkanes were eluted with 5 ml hexane before reducing under pressure, collected in 4 ml vials, and reduced to dryness under nitrogen. They were then re-dissolved in 1 ml hexane; 180 µl of the sample was transferred to a vial with an insert, after which 20 µl of 100 mg/l deuterated tetracosane and androstane mixture was added as an internal standard. The sample was then analysed using an Agilent 6890 N gas chromatograph (GC) interfaced with a 5973 MSD mass spectrometer (MS) with an HP-5 (5% phenyl methyl siloxane) fused silica capillary column (30 m length x 0.25 mm i.d. x 0.25 µm film thickness). The oven was kept at a constant temperature of 35 °C for 6 min, increased to 300 °C at 5 °C min^{-1} and then held for 20 min. The GCMS was operated at 70 eV in full scan mode (*m/z* 50–500 amu). The compounds were identified based on their retention time, *m/z* ratios, authentic standards and online libraries (NIST and the Lipid Library). The detection limit of compounds ranged from 0.1 up to 1 ng/g. Recovery of the deuterated hexatriacontane ranged from 75% to 85%.

3. Results

3.1. Lithology

Core KP1A consists primarily of peat with occasional silt and sand layers of different thicknesses. The core could be roughly divided into five sections showing differences in physical appearance based on its colour, sand/silt, degraded and amorphous composition, and presence of distinct rootlets and leaf blades (Fig. 2). While the minerogenic component is higher in the lower sediments, the upper horizons consist of organic components such as decomposed plant matter, rootlets and occasionally leaf blades (220–100 cm). The core was also water-logged towards the top (100–0 cm), whereas the lower intervals were more dry and compact. The bottom of the core represented a hard silty-sand interval (starting around 395 cm) that could not be penetrated with the peat borer beyond 400 cm. It most likely represents a weathered surface or bedrock.

3.2. Chronology

The KP1A ^{14}C ages occur in stratigraphic sequence and are indicated in Table 1. The calibrated ages for individual ^{14}C age in Table 2 were derived using IntCal20 in Clam, which provided a range with 95% probability. The post-bomb calibration curve NH3 was applied to calibrate the modern ^{14}C age (pMC value). The model derived minimum, maximum, median and mean ages provided by the BACON program after excluding the outliers and are indicated in Appendix 1. The model-derived median ages were used to define boundaries in the core to discuss the multi-proxy data.

The ^{14}C age generated for the sample from the weathered bottom at around 399 cm was automatically rejected by the BACON model using the student's *t*-distribution. The bottom layer was a weathered sandy interval with lower C content which increases the chances of error during ^{14}C dating. The linear sedimentary rate (LSR) in cm yr^{-1} was calculated from the age-depth profile and showed two sedimentation regimes in the peat sequence. The lower portion of KP1A (400–225 cm) has an average LSR of 0.08 cm yr^{-1} spanning c. 3023–625 cal yr BP and the upper part (224–0 cm) have an average LSR of 0.44 cm yr^{-1}.

3.3. Chemical proxies

TOC values fluctuate between 10% (376 cm; 2766 cal yr BP) and 42% (176 cm; 421 cal yr BP) with an average of 25% (Fig. 3). TOC increases steadily from 10% (400 cm; c. 3023 cal yr BP) to about 33% (284 cm; 1401 cal yr BP) and then decreases to 12% (225 cm; c. 625 cal yr BP) before reaching the core maximum. TOC remains relatively stable before gradually decreasing to 16% at the surface. Change in TOC levels in the core is expressed as mass accumulation rate (MAR) calculated according to (Meyers and Teranes, 2002),

$$MAR = DBD \times LSR \left(g.cm - ^{2}.yr^{-1}\right) \quad (1)$$

where DBD is the dry bulk density and LSR is the linear sedimentation rate.

The TOC MAR starts low at 0.3 g cm^{-2} yr^{-1} and varies less for the bottom half of the core. MAR increases when sedimentation increases to

Table 1
Accelerator mass spectrometry radiocarbon dates for the Kapsabet peat deposit. (calibrated age range generated using IntCal20 with 95% probability).

Lab ID	Depth (cm)	^{14}C Age years BP (conventional age)	Error	Age cal yr BP (95% probability)
Poz-72905	75	102 (pMC)	0.33	Modern (ca. 1955 CE)
Poz-75146	125	115	30	11–268
Poz-72906	175	230	30	0–419
Poz-75147	225	535	30	514–625
Poz-72907	275	1410	30	1289–1351
Poz-75148	325	1880	30	1716–1868
Poz-72890	375	2650	30	2729–2845
Poz-75149	399	3925	30	4246–4504

Table 2
Summary of paleoenvironmental proxies and their interpretation.

Environmental proxy	Background	Interpretation	Ratio
TN and TOC (Meyers and Teranes, 2002)	Shows available nitrogen and carbon content in the sediment.	High values suggest a high input of OM and good preservation.	
C/N ratio (Meyers, 1994)	Indicates OM sources, productivity, and degradation.	High values suggest terrestrial input. Low values imply poor preservation from microbial/ chemical degradation or low organic input.	
δ^{13}C (Meyers and Teranes, 2002; Talbot and Lærdal, 2000)	Shows past productivity and OM sources	High values indicate high productivity and terrestrial OM. Higher (enriched) values imply high degradation or lack of organic input.	
δ^{15}N (Högberg, 1997; Robinson, 2001)	Biochemical reactions such as nitrification and ammonification	The higher the values indicate high nitrification.	
Carbon Preference Index - CPI (Meyers and Ishiwatari, 1995)	Indicates immature source rocks with significant input of land-derived OM. C_{21}-C_{25} alkanes characterize emergent plants; C_{27}-C_{35} alkanes characterize terrestrial OM.	High values indicate higher terrestrial plant sources and better preservation of OM.	$CPI = \frac{1}{2}\left(\frac{(C_{25}+C_{27}+C_{29}+C_{31}+C_{33})}{(C_{24}+C_{26}+C_{28}+C_{30}+C_{32})}+\frac{(C_{25}+C_{27}+C_{29}+C_{31}+C_{33})}{(C_{26}+C_{28}+C_{30}+C_{32}+C_{34})}\right)$
Average Chain Length - ACL (Cranwell et al., 1987)	Plants produce long-chain leaf waxes in warmer conditions.	High values suggest warm conditions.	$ACL = \frac{[25(nC_{25})+27(nC_{27})+29(nC_{29})+31(nC_{31})+33(nC_{33})]}{(nC_{25}+nC_{27}+nC_{29}+nC_{31}+nC_{33})}$
Aquatic Plant index - P_{aq} (Ficken et al., 2000)	Mid-chain alkanes dominate aquatic plant waxes.	Higher values suggest more aquatic plant input.	$Paq = \frac{(C_{23}+C_{25})}{(C_{23}+C_{25}+C_{29}+C_{31})}$
Terrigenous Aquatic Ratio - TAR (Bourbonniere and Meyers, 1996)	Emergent and terrestrial plant waxes have long-chain alkanes.	Higher values suggest more terrestrial/ emergent plant input.	$TAR = \frac{(C_{27}+C_{29}+C_{31})}{(C_{15}+C_{17}+C_{19})}$

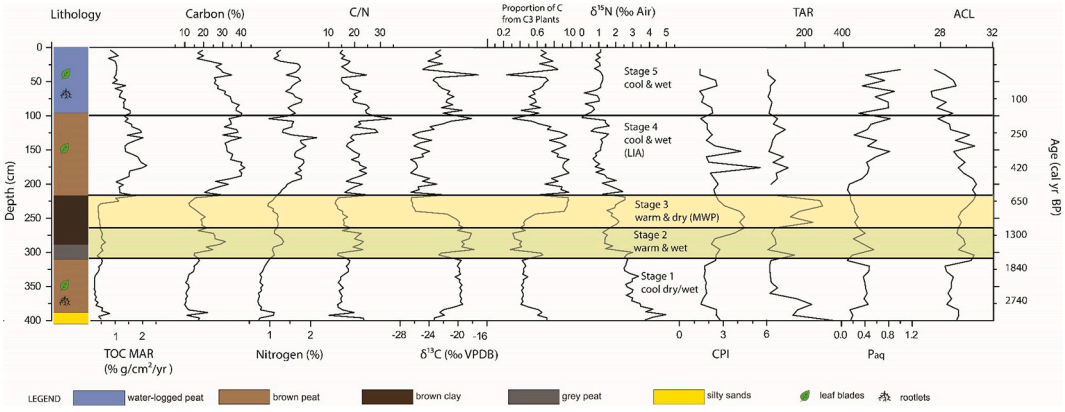

Fig. 3. Elemental, stable C and N isotopes and n-alkane ratios (CPI, TAR, P_{aq}, and ACL) in the Kapsabet (KP1A) peat sequence. The core is divided into 5 stages (St 1–5) based on the geochemical proxies. LIA. Little Ice Age, MWP – Medieval Warm Period.

about 3.0 g cm^{-2} yr^{-1} at 226 cm. After that, TOC MAR gradually reduces upwards in the core.

TN values vary between 0.7% and 2.2%, with an average of 1.3% (Fig. 3). TN maximises between 100 and 200 cm. The bottom of the core from 400 to 200 cm shows a gradual increase, whereas the upper part (100–0 cm) shows more variability superimposed on a gradually decreasing trend. C/N fluctuates between 10 and 34 (Fig. 3) and averages c. 18. The C/N values start with a sharp decrease before rising steadily up the core with intermittent spikes.

The δ^{15}N values decrease steadily up the core, starting from a high of 5‰ at the bottom to 1‰ at the top (Fig. 3). The δ^{15}N values do not share the same trend as δ^{13}C. The δ^{13}C values increase at the bottom of the core from −23‰ to −19‰ (Fig. 3) and remain in that range to about 270 cm (c. 1257 cal yr BP), after which the δ^{13}C values increase slightly, followed by a decrease to −26‰ (225 cm; c. 625 cal yr BP). The δ^{13}C values increase to about −18‰ around 100 cm (c. 188 cal yr BP) before

steadily decreasing to about −22‰ and finally increasing near the top at 40 cm.

To broadly gauge the relative proportions of C input from C3 and C4 vegetation in Kapsabet Swamp, a mass balance equation was used (Boutton et al., 1998; Gillson et al., 2004; Baker et al., 2014).

$$\delta^{13}C_{peat} = (\delta^{13}C.C4\ plants)x + \delta^{13}C.C3\ plants\ (1-x) \quad (2)$$

where $\delta^{13}C_{peat}$ = bulk stable isotope composition of organic matter in the sample; regional isotopic values of C3 (−27.5‰) and C4 (−13.2‰) vegetation from the region (Muzuka, 1999); x is the proportion of C input from C4 plants and 1-x is the proportion of C from C3 plants. The end-member value used in mixing models is crucial (Castañeda et al., 2009). Therefore, values suggested from the African savannah (Gillson et al., 2004) were used in this equation. The data indicate a high proportion of C input from C3 vegetation and is mostly >0.5; the maximum input occurs in the mid-section between 250 and 100 cm (Fig. 3).

CPI values in the KP1A core range between 1.37 and 5.54, with an average of 2.44 (Fig. 3). The ratio starts at about 3 at the bottom of the core then reduces slightly up to 370 cm (c. 2667 cal yr BP) before increasing gradually to about 4.5 at 260 cm (c. 1117 cal yr BP). CPI gradually reduces at the top of the core. The TAR values range from 2.76 (32 cm) to 356 (400 cm) and the average is 110. TAR values generally decrease core upwards. The P_{aq} values start low at the bottom and increase gradually core upwards. In general, the bottom half has values <0.5 and the top half has values >0.5. ACL ranges from 27.3 to 30.1, with the average being 29.2. ACL starts at about 29 at 400 cm (c. 3023 cal yr BP) and maintains the same value with minor variations up to the surface with an overall decreasing trend.

4. Discussion

4.1. The analytical rationale for paleoclimate proxies

The absence of instrumental records that go beyond 200 years constrains the reconstruction of long-term palaeoenvironmental changes. Researchers, therefore, focus on alternate methods related to the physical, biological, and chemical characteristics in sedimentary archives to reconstruct paleoclimate changes (Bruckner, 2006). The combination of bulk and molecular characteristics such as elemental concentrations, stable isotopes and biomarker data provide highly resolved details about primary production, delivery and preservation of OM in the catchment (Meyers, 2003; Peters et al., 2005; Castañeda et al., 2009; Castañeda and Schouten, 2011). Table 2 summarises a list of commonly used bulk and molecular proxies and their usefulness in interpreting paleoenvironmental changes.

4.2. Age-depth model

With a high C content and rapid deposition, ^{14}C dating in bulk OM can be challenging due to contamination from plant macrofossils, charcoal, and other sources that are older than the deposits being examined (Björck and Wohlfarth, 2002; Blaauw et al., 2011). Fossils can be reworked or transported from older horizons, which complicate sediment chronology reconstruction (McKinney et al., 1995; Verschuren, 2004). In particular, the input of weathered old carbon varies through time, and the low carbon content in the minerogenic intervals makes it hard to constrain the ages (Felton et al., 2007). However, with a high C content and a rapid deposition rate, peatlands typically yield accurate chronologies based on bulk C content. In this study, the bulk C measurements in the Kapsabet peat sequence extend from c. 3023 cal yr BP to the present (Fig. 2; Table 1). The sediment accumulation rate is slow (0.08 cm yr^{-1}) from 3023 cal yr BP onwards but abruptly increases at c. 625 cal yr BP (0.44 cm yr^{-1}, 225 cm), coinciding with the deposition that follows the Little Ice Age (LIA; Fig. 3). The low sedimentation rate in the deeper sediments is perhaps due to compaction, catchment vegetation, and soil stabilisation, leading to lowered quantities of terrestrial sediments being transported into the swamp. The sedimentation rate changes particularly after the LIA coinciding with cooler and wetter conditions in the recent past. This drastic change in sediment accumulation rate around the LIA in East Africa is documented by lithological and microfossil changes in the Loboi Swamp, Lakes Baringo, and Naivasha within the Kenya Rift and in other parts of eastern equatorial Africa. These data suggest a wet period from c. 1270–1850 CE (Verschuren et al., 2000; Driese et al., 2004; De Cort et al., 2013; Buckles et al., 2016).

4.3. Paleoenvironmental reconstruction

The highland peat sequence from Kapsabet can be divided into five palaeoclimatic stages, as discussed below, based on distinct changes in the sediment layers and their proxy characteristics. The lithological changes, TOC, C/N, $\delta^{13}C$, $\delta^{15}N$ CPI, TAR P_{aq} and ACL data provided a temporally broad indication of changes in the environment driven by natural and, more recently, by anthropogenic factors.

In Stage 1 (400 to 310 cm, c. 3023–1670 cal yr BP), the carbon accumulation rate was relatively low compared to the later stages; OM preservation was low as reflected in CPI, TOC MAR and TOC values. The C/N ratio suggests a mix of aquatic plants and humified terrestrial OM. $\delta^{15}N$ declines upwards through the core, in tandem with a general, observed enrichment of $\delta^{15}N$ in the mineral fraction of soils as a consequence of progressive decomposition of plant residues (Tiunov, 2007), but which likely reflects, in reverse order, a progressive change from a forested to an established open woodland landscape (cf. Martinelli et al., 1999) from 3023 to c. 150 cal yr BP. Confidence in this interpretation relates to the fact that the average ^{15}N value for tropical tree foliage is 4.7 ± 2.1‰ (Martinelli et al., 1999), and coupled with the high sedimentation rate in the swamp that limits OM degradation and humification, it can be inferred that there is some retention of long-term foliage dynamics in the sediments. Further, the change is supported by the TAR values, which reflect at the beginning a high input of terrigenous OM, which progressively declines with time. Initially, high TAR and negative $\delta^{13}C$ values at 3023 cal yr BP decline steeply to low values at c. 2300 cal yr BP (with a positive TAR peak at c. 1700 cal yr BP) that are maintained to c. 1100 cal yr BP, which inversely correlates with P_{aq}. This trend reflects a progression from a dry to a wet period with maximum wetness between 2737 and 1840 cal yr BP, and which terminates with a dry episode at c. 1670 cal yr BP. This trend is also supported by more negative $\delta^{13}C$ signals, signifying higher productivity and/ reduced OM degradation. As indicated by the low ACL value, the climate was likely cool, and the system was generally stable (invariant TAR, P_{aq}, $\delta^{13}C$, TOC, TN and C:N ratio) from 2737 to 1670 cal yr BP when the drier and cooler episode occurred. This trend contrasts with the reported fluctuations in lake level in Lake Victoria and vegetation in the western catchment area from c. 5900 to 1400 cal yr BP (Nakintu and Lejju, 2016). The dry event marking the end of this period correlates with fires that peaked between 1700 and 1450 cal yr BP as deduced from a core recovered from deep water in Lake Victoria (Battistel et al., 2017), at Sacred Lake on Mount Kenya (Konecky et al., 2014) and with droughts reported by Ssemmanda et al. (2005) in western Uganda extending from c. 1800–1700 cal yr BP based on pollen reconstruction. While fires were identified by Battistel et al. (2017) centered c. 2000 cal yr BP, and drought was inferred at 2500 cal yr BP in the Cherangani Hills (Opiyo et al., 2019), conditions in the highland Kapsabet swamp implies the prevalence of wetter conditions.

During Stage 2 (310 to 265 cm, c. 1670–1187 cal yr BP), the accumulation rate for OM was low according to the TOC MAR values. This period was marked by higher TOC, TN and C:N ratios, more positive $\delta^{13}C$ values, negative $\delta^{15}N$ values, and lower P_{aq} than Stage 1. The higher values for TOC, TN and C:N ratios, more enriched $\delta^{13}C$ values and low TAR values suggest high productivity in the swamp contributing to a dominant in situ OM source, coupled with still important OM inputs

from the catchment, more so towards the end of the Stage as indicated by the increasing CPI and C/N values. There is also increased variability in proxy signals, reflecting a fluctuating climate but still predominantly wet with the in situ contribution of OM as reflected by the low TAR and high P_{aq} indices and relatively warmer conditions than Stage 1 based on the ACL values. In general, Stage 2 was a warm and variably wet period with high productivity and OM input derived mainly from aquatic sources but also with important terrestrial source inputs. This variability observed is consistent with the Lake Naivasha record, which shows a fluctuating lake regime of low to intermediate lake levels (Verschuren, 2001), but contrasts with western Uganda, where it was generally drier between 1300 and 1000 cal yr BP (Ryves et al., 2011). It is likely the warming reported by Battistel et al. (2017) in the low altitude areas of the catchment during Stage 1 was extending further up the highlands, concomitant with a pronounced increase in inter-decadal to centennial-scale climate variability in the lowlands and highlands within the catchment (Russell and Johnson, 2005; Marchant et al., 2018 and references therein).

In Stage 3 (265 to 225 cm, c. 1187–625 cal yr BP), the low TOC, TOC MAR and TN suggest low OM accumulation or a high degradation rate. The reduced C/N values suggest degradation coeval with negative $\delta^{13}C$ values. This inference is further supported by the declining CPI values towards the upper part of this stage, confirming poor preservation. The OM source is mainly of terrestrial origin, as indicated by the high TAR, reducing P_{aq} trends and negative $\delta^{13}C$ values. This is consistent with the $\delta^{13}C$ mass balance, which indicates the proportion of C inputs from C3 plants that maximise and continue into Stage 4. C3 plants have an advantage over C4 grasses. They can outcompete C4 grasses when there is plentiful water available to the plants, even if temperatures are high and the yearly precipitation is low (Ehleringer et al., 1997). Also, C4 sedges (Cyperaceae) are common in the swamp, and an increase in $\delta^{13}C$ values does not necessarily mean an increase in C4 grasses. Although warm and arid conditions have been suggested to increase the C4 plant cover (Edwards et al., 2010; Schefuß et al., 2003), there is limited evidence for it in eastern Africa (Levin, 2015). Notably, ACL increased steadily throughout this zone, suggesting gradual warming. This is consistent with the fact that Stage 3 spans the late Holocene Medieval Warm Period (c. 900–1300 CE; 1100 to 700 cal yr BP). This warm, dry climate is similar to that which has been inferred from Lake Victoria cores (Stager et al., 2005) and other regions of East Africa (Verschuren et al., 2000; Russell and Johnson, 2005; Ssemmanda et al., 2005; Nakintu and Lejju, 2016; De Cort et al., 2018; Marchant et al., 2018), and is characterized by muted interdecadal to centennial-scale variability relative to Stage 2.

The beginning of Stage 4 (225 to 100 cm, c. 625–188 cal yr BP) is marked by a shift in LSR from 0.08 cm yr^{-1} to 0.44 cm yr^{-1}, which coincides with the start of the LIA in East Africa. This Stage captures the entirety of the LIA. Abrupt and sharp increases in TOC, TOC MAR and C:N ratio coupled with more negative $\delta^{13}C$ and $\delta^{15}N$ suggest a significant but short-lived in-wash of terrestrial-derived OM into a generally dry swamp, which then became progressively wet. The mass balance data shows predominantly C3 derived input that declines near the top. The change in sedimentation rate that marks the start of the LIA correlates with a sharp decline in TAR values and a decline in $\delta^{15}N$, suggesting a shift to wet conditions as reflected by other records from East Africa (Verschuren et al., 2000; Driese et al., 2004; De Cort et al., 2013; Buckles et al., 2016). More generally, during this period, all the proxies, except the TAR, exhibit their largest variability in the core, indicating that the climate and environment of the time were highly variable and unstable in relation to the preceding and successive periods. The low variability in the TAR suggests that the balance between terrestrial and aquatic sources of OM did not change much, though the other proxies such as $\delta^{13}C$, C:N ratios, and CPI probably reflect significant periodic changes in the vegetation structure within the swamp and its surrounding catchment in response to strong climatic and hydrological variability. It is also inferred that the swamp never dried out completely, as reflected by the P_{aq} values. TOC increases to its highest value (c. 40%) at 175 cm before it steadily reduces, signaling a period of increased productivity followed by a general slowdown. C/N ratios increase erratically to suggest a slowdown in OM degradation. The $\delta^{13}C$ values are ^{13}C-depleted and indicate terrestrial C_3 input. The high CPI confirms the terrestrial origin of OM and the overall good preservation of sedimentary OM during this stage. High P_{aq} and low TAR values suggest that OM input is most likely derived from aquatic sources. Based on the low ACL values, this period was likely as cool as Stage 1 but not as stable (more temporally variable) with respect to precipitation and hydrological conditions.

Stage 5 (100 to 0 cm, c. 188 cal yr BP to present) is characterized by reduced TOC, TN, and C/N values, suggesting a progressive reduction in productivity. The variable climate, hydrology and environmental conditions observed in Stage 4 continue through this stage, but it is slightly muted relative to Stage 4 (except for P_{aq}, which maintains a similar magnitude of variability). Decreasing trends in ACL values suggest a gradual cooling, extending from the LIA. High P_{aq} indicates a more significant input of aquatic-derived sources, most likely from submerged/floating macrophytes (cf. Ficken et al., 2000). The decrease in ACL values coeval to lighter $\delta^{13}C$ values implies a change in temperature and input of aquatic plants. There is an increase in the proportion of C3 input, although it is less than the preceding two stages; the proportion of C from C3 plants declines (0.28) before increasing again, showing an overall variability in the proportion of C from C3 and C4 derived organic matter during this stage. Likely, the relatively depleted ^{15}N- signal in the upper 100 cm (from c. 150 cal yr BP to present) in the core suggests an open N cycle that is typical for tropical regimes as suggested by Martinelli et al. (1999), and which allows for losses due to denitrification, frequent forest fires, and changes in atmospheric conditions (Zech, 2006). Such changes are coeval with human activities, which coincide with land-use practices such as agriculture and deforestation. This period coincided with rapid demographic changes brought about by the European colonisation of East Africa. Furthermore, a sharp increase in the indigenous and immigrant population coincided with the degradation of the landscape, including deforestation and extensive soil erosion, as sedentary farming practices increased in the whole region, particularly the lowlands (Marchant et al., 2018 and references therein).

4.4. The human-environment tangle

In Africa, the relationships between climate, environment and human behaviour have been influenced by a combination of natural forcings (high-latitude ice distribution, sea surface temperature, and low-altitude orbital forcings) that affected the vegetation cover and moisture availability which played an important role in the human-environment interactions (Levin, 2015; Marchant et al., 2018; Chritz et al., 2019). The general reduction of moisture in East Africa from the mid-Holocene onwards coincided with the rise of human impacts, which have been traced in the pollen sequences and fire records (Hamilton et al., 1986; Marchant et al., 2018; Opiyo et al., 2019). However, anthropogenic impacts make the separation of natural vs. human-induced changes sometimes challenging to unravel. For example, droughts have been characterized based on the high number of Gramineae pollen and charcoal (e.g., Kiage and Liu, 2006; Opiyo et al., 2019). However, a similar trend has been indicated to represent human activities such as agriculture or pastoralism (Marchant et al., 2018 and references therein). Most sites in the Lake Victoria catchment are less likely to be impacted by such confounding evidence due to the delayed adoption of iron technology (Hamilton et al., 1986; Kiage and Liu, 2006). Besides, many of these remote and isolated locations (such as the study area) have had limited human intervention until the last few centuries, and that too, after colonisation.

Peatlands are nevertheless vulnerable to land-use changes and human activities. In recent years, urban encroachment of peatlands has led to their destabilisation, which has enhanced OM degradation, soil erosion, loss of biodiversity, and enhanced greenhouse gas emissions

(Posa et al., 2011; Grzybowski and Glińska-Lewczuk, 2020). Although such dramatic changes are absent in the recent past, fires and pollen assemblages have been reported that are of anthropogenic origin and traced back as early as the mid-Holocene epoch in Kapkanyar Swamp (~4300 yrs.; Opiyo et al., 2019), Ahakagyezi Swamp (~4800 yr BP; Hamilton et al., 1986; Taylor, 1990) and Muchoya Swamp (~2500 yr BP; Taylor, 1990) implying deforestation and agriculture practices in the catchment. For example, Vincens (1989) reported *Elaeis guineensis* (wild oil palm) in the pollen record from Masoko, indicating cultivation. More intensive forms of agriculture and cultivation in the different interlacustrine regions were initiated by the Bantu people (Hamilton et al., 1986) as early as 2000 yr BP since the Masai have traditionally been pastoralists (Galaty, 1993). These records indicate that the degradation of the environment by man (although limited) occurred reasonably early in the region. Moreover, it was local rather than regional ecological changes that affected the migration of early herders (and settlers) into the rift valley lake systems as the Lake Victoria lowlands c. 4000 yr BP (Chritz et al., 2019).

Anthropogenic influence of human activities in these studies had mainly been traced from the record of arboreal pollen assemblages and microscopic charcoal representing fires associated, e.g., with agricultural or domestic activities. These proxies not just record the mere presence of people but provide a semi-quantitative appraisal of various land-use practices. However, pollen from most cultivated plants in the East African region remains unknown (Msaky et al., 2005). Pollen could also be transported from distant places or undergo severe degradation under humid/hot conditions after deposition. Moreover, pollen is also a poor proxy for tracing subtle changes in vegetation – these challenges make land-use interpretations based solely on pollen contentious in East Africa (Kiage and Liu, 2006; Marchant et al., 2018). Although Kapsabet Swamp is a small, remote and isolated location, it is a promising geoarchive. In fact, several archeological sites occur east of the Nandi Hills (Marchant et al., 2018) and to the south (Chritz et al., 2019), providing other possible lines of investigation for studying human-environment interactions (Levin, 2015; Boivin et al., 2016; Chritz et al., 2019; Jha et al., 2020) in the highlands of the Lake Victoria catchment.

4.5. Regional context

Mayewski et al. (2004) compared over 40 paleoclimate records from around the globe. They recognised six periods of major climatic shifts during the Holocene at 9000–8000, 6000–5000, 4200–3800, 3500–2500 (Stage 1 in our record starting from 3023 cal yr BP), 1200–1000 cal yr B.P. (early Stage 3 in our record), and 600–150 cal yr B.P. (Stage 4 in our record). Broadly, overarching palaeoclimate studies in Lake Victoria suggest that during the last 4000 cal yr BP, the climate became more seasonal with lower precipitation than during the early and mid-Holocene epoch (Talbot and Lærdal, 2000; Marchant et al., 2018). Further, Kiage and Liu (2006) indicated anthropogenic imprints as indicated by the steady decline in tree cover in western East Africa, which coincided with extensive soil erosion associated with the expansion of agriculture and land clearance that started c. 3000 cal yr BP (Table 3). The overlap between changes inferred from different sites in the Lake Victoria catchment (or even beyond) suggests a causality and that the late Holocene climatic changes were predominantly regional. The following discussion is partly framed using the Mayewski et al. (2004) context of global Holocene climate change.

During Stage 1 (3023–1670 cal yr BP), the Kapsabet record sees the area progressively changing from drier to wetter conditions with increased precipitation from 2740 to 1840 cal yr BP. This ties in with a Lake Victoria core that shows a significant extension of high altitude dry montane forest with *Podocarpus* and *Juniperus procera* reaching a maximum at c. 1700 cal yr BP, with greater rainfall inferred at high altitude sites (Ssemmanda and Vincens, 2002). The early part of the Kapsabet record (3023 to 2737 cal yr BP) reflects pronounced aridity in East Africa between 3500 and 2500 cal yr BP (Mayewski et al., 2004)

Table 3
Summary of the regional environmental changes indicated in previous studies and changes inferred in the highland Kapsabet swamp from Kenya (East Africa).

Stage	Study	Location	Inferred climatic condition
Stage 1 (c. 3023–1670 cal yr BP)	*This study*	*Kapsabet*	*Cool dry/wet climate*
	Talbot and Lærdal, 2000; Marchant et al., 2018	East Africa	Seasonal climate with less precipitation than early and mid-Holocene
	Kiage and Liu, 2006	Western East Africa	Extensive soil erosion and decline in tree cover
	Nakintu and Lejju, 2016	Western L. *victoria*	The fluctuation of lake level in L. Victoria and vegetation cover
	Battistel et al., 2017	L. Victoria	Dry events peaked between 1700 and 1450 cal yr BP
	Opiyo et al., 2019	Cherangani Hills (N of Kapsabet)	Drought not reflected in our study
	Ssemmanda and Vincens, 2002	L. Victoria	More rain in high altitudes than low latitude
	Mayewski et al., 2004	East Africa	Pronounced aridity
	Johnson et al., 1991; Halfman et al., 1994	L. Turkana (North of Kapsabet)	Arid climate
	Konecky et al., 2014	Mt. Kenya (NE of Kapsabet)	Arid climate
	Verschuren et al., 2009	L. Challa (SE of Kapsabet)	Arid climate
Stage 2 (c. 1670–1187 cal yr BP)	*This study*	*Kapsabet*	*Wet climate; warmer than stage 1*
	Verschuren, 2001	L. Naivasha	Fluctuating low and intermediate lake levels
	Ryves et al., 2011	Western Uganda	Dry climate
	Russell and Johnson, 2005	Lake Albert (W of Kapsabet)	Variable climate, mostly wet
	Battistel et al., 2017	low altitude Lake Victoria basin	Warm climate
	Stager and Johnson, 2000; Talbot and Lærdal, 2000	L. Victoria	Increased aridity
Stage 3 (MWP) (c. 1187–625 cal yr BP)	*This study*	*Kapsabet*	*Warm and dry climate*
	Mayewski et al., 2004	East Africa	Major climate shift
	Marchant et al., 2018	L. Victoria	Dry events
	Stager et al., 2005	L. Victoria	Warm and dry climate
	Verschuren et al., 2000	Nakuru (N of Kapsabet	Warm and dry climate
Stage 4 (LIA) (c. 625–188 cal yr BP)	*This study*	*Kapsabet*	*Cool with variable precipitation*
	Verschuren et al., 2000	Uganda-Congo border	Humid/dry climate
	Buckles et al., 2016	L. Challa (SE of Kapsabet)	Dry climate; Droughts (?)
	Russell and Johnson, 2005; Stager et al., 2005; Stager and Johnson, 2007; Verschuren and Russell, 2009	L. Victoria	Wet climate
	Verschuren et al., 2000	L. Nakuru	Wet climate
Stage 5 (c. 188 cal yr BP to present)	*This study*	*Kapsabet*	*Alternating wet and dry climate*
	Ssemmanda et al., 2014	Southwestern Uganda	Multiple wet periods (3)

(*continued on next page*)

Table 3 (*continued*)

Stage	Study	Location	Inferred climatic condition
	Nicholson, 2000; Verschuren et al., 2000; Ryves et al., 2004	East Africa	Arid phase
	Verschuren et al., 2002; Marchant et al., 2018	East Africa	Significant human impact on climate

that ended 240 years later. Mayewski et al. (2004) relate this arid period to a decline in solar output based on observed maxima in $\Delta^{14}C$ residuals (Stuiver et al., 1998) and ^{10}Be concentrations in the GISP2 ice core records (Finkel and Nishiizumi, 1997). Within East Africa, coincident arid events are recorded, for example, between c. 2200 yr BP and 1700 yr BP in Lake Turkana cores (Johnson et al., 1991; Halfman et al., 1994), at Sacred Lake on equatorial Mount Kenya just before 1700 cal yr BP (Konecky et al., 2014), the crater Lake Challa on the northern foot slopes of Mount Kilimanjaro from 2000 to 1600 cal yr BP (Verschuren et al., 2009), and between 2050 and 1850 cal year BP in Lake Edward, on the Uganda-Congo border (Russell and Johnson, 2005).

Stage 2 (1670–1187 cal yr BP) was warmer than Stage 1 and marks a period when climate variability became markedly enhanced in the eastern highlands of the Lake Victoria catchment, but with a predominance of wet over dry episodes. This observation is supported by the pronounced century-scale variation from 1500 to 900 cal yr BP observed west of Lake Victoria, in Lake Albert on the Uganda-Congo border (Russell and Johnson, 2005). However, this period does not fall into a "major climate shift" category outlined by Mayewski et al. (2004). Nevertheless, the Lake Victoria core records show some increased aridity, most likely due to deforestation after 1400 cal yr BP (Stager and Johnson, 2000; Talbot and Lærdal, 2000). Russell and Johnson (2005) have suggested that based on a review of tropical lake records, the observed variability is most likely related to the Indian Ocean monsoon system rather than to solar forcings or other mechanisms that drive climate dynamics.

The key features of Stage 3 (1187–625 cal yr BP) are that it was characterized by a warm, dry climate with a muted inter-decadal to centennial-scale variability relative to Stage 2. It also coincided with the Medieval Warm Period, which started towards the end of Stage 2 at Kapsabet (c. 900–1300 CE; 1100 to 700 cal yr BP). This period falls within the Mayewski et al. (2004) "major climate shift" of 1200–1000 cal yr BP attributed to a low-latitude aridity response to high-latitude cooling. Many records document the Medieval Warm Period in the East Africa region (Marchant et al., 2018), but the onset, duration and cessation vary with site-specific climate dynamics, sedimentation characteristics, and the temporal resolution of the geochronological controls. For example, Lake Victoria experienced two low water level events from 820 to 760, and 680 to 660 cal yr BP (Stager et al., 2005), out of phase with the 1200–1000 cal yr BP "period of major shift", implying that regional climate systems dominated over high-latitude cooling effects in this area. Similarly, studies in nearby Lake Nakuru also reflect a warm and dry climate between 1000 and 680 cal yr BP (Verschuren et al., 2000).

Stage 4 (625–188 cal yr BP) in the Kapsabet record captured the entirety of the LIA and was characterized by a cool (as cool as Stage 1), highly variable and unstable climate, hydrology vegetation structure and composition in its catchment. Various studies show that east of Lake Victoria, and as far as the Indian Ocean coast, the LIA was relatively humid, albeit with intervening dry episodes (e.g., Verschuren et al., 2000; Buckles et al., 2016). In contrast, to its west along the Uganda-Congo border and the Ruwenzori Mountains, it was comparatively dry, with some intense droughts, following an initially wet start (e.g., Russell et al., 2007; Tierney et al., 2013). During this period, Lake Victoria experienced lake level minima c. 680–660, 370–340, and 220–150 cal yr BP, and maxima from 600 to 400 and 300–250 cal yr BP that match the Naivasha record (Verschuren et al., 2000). Stager et al. (2005) postulated that an in-phase relationship between prolonged sunspot minima and high lake levels in East Africa indicated a causal link between the two, but this remains a hypothesis since those relationships reversed their signals c. 200 years ago. They are further confounded by the effects of the El Niño–Southern Oscillation (ENSO) and Indian Ocean Dipole, which also lead to lake level rise, and lack of clarity on the influence/interaction between solar radiation changes and the position of the Inter-Tropical Convergence Zone. Further, the migration (linked to ENSO during high latitude cooling) of the Congo Air Boundary (CAB) where Atlantic and Indian Oceans moisture meets likely played a role. This was most likely the case during the main phase of the LIA (1400–1750 CE; 600–250 cal yr BP), resulting in contrasting records from the sites to the east (wet) and west (dry) of the CAB (Russell and Johnson, 2007; Verschuren and Russell, 2009). For example, studies in nearby Lake Nakuru showed a relatively wet period extending from 680 to 150 cal yr BP (Verschuren et al., 2000).

Stage 5 (188 cal yr BP to present): The climatic regime in this period is similar to the LIA, characterized by alternating wet and dry episodes but with a relatively muted variability. Three wet episodes have been deduced from pollen studies of a core from Lake Chibwera, a relatively low altitude site in southwestern Uganda c. 1820–1830, 1865–1890 and 1962 to 2000 (Ssemmanda et al., 2014). A widespread arid phase characterized the early part of this period from 150 to 100 cal yr BP (Nicholson, 2000; Ryves et al., 2004; Verschuren et al., 2000). Here, in contrast to the LIA, there is a positive relationship between sunspot maxima and high lake levels (Stager et al., 2005). Human activities became highly significant with regard to the modification of the environment in the Lake Victoria catchment, particularly the lowlands (see Verschuren et al., 2002; Marchant et al., 2018;). Kiage and Liu (2006) indicated that the steady decline in tree cover in western East Africa coincided with extensive soil erosion associated with the expansion of agriculture and land clearance. The Kapsabet swamp was likely impacted, but our proxies could not discriminate between anthropogenic and natural factors. Widespread changes in terms of human migration in the Lake Victoria catchment began in the region, with the settling of Masai tribesmen who came from the northern territories with their cattle 500 years ago (Galaty, 1993). Agricultural expansion followed as large swathes of the lowlands were settled. These effects, though, are more evident in the lowland areas of Lake Victoria's catchment.

During the late Holocene, there have been significant changes in the Kapsabet record related to solar forcing, high latitude cooling events, shifts in regional climate systems, and modification of local microclimate. Solar variability remains a major driver through the five Stages, albeit with as yet unresolved forcing pathways as noted for the last millennium. While the climate drivers have been mostly attributed to direct solar variability as discussed above, it has been shown that half-precessional forcing at the equator has a major effect on rainfall and hydrology at millennial timescales (Olago et al., 2000; Verschuren et al., 2009) and that the higher precessional harmonics also contribute to mean trends over long timescales (Olago et al., 2009) and higher frequency hydrological variability (Olago et al., 2000). This aspect likely played an underlying role in the variability observed in the Kapsabet and other records from East Africa from 1500 cal yr BP to the present. Many authors have noted that the spatial decadal variability of rainfall and its amounts in East Africa over the past 200 years may be related to variations in the strengths and the degree and phase of interaction between the ENSO, the Indian Ocean Dipole, deep westerly airstreams from the Atlantic, and the Congo air mass (e.g., Nicholson, 2000; Olago et al., 2009). Such relationships were also affected by the steep topographical gradients and large water bodies in the region, coupled with land cover changes (Olago et al., 2009).

5. Conclusions

Generalising climate inferences based on a single sedimentary archive is not always straightforward. In the present study, the Kapsabet Swamp deposit was well-preserved and could be related to regional climate changes and their impacts through the late Holocene. Several well-established geochemical indicators of peat-forming processes were used and related to changes in OM source inputs, preservation, and diagenetic alteration to reconstruct paleoenvironmental conditions in this highland swamp, Lake Victoria catchment. Specific peat characteristics can be correlated and contrasted with changes recorded within Lake Victoria and other regional studies to distinguish the ongoing natural versus anthropogenic environment in east Africa for the last c. 3000 years.

The TOC MAR indicates two sedimentation regimes in the Kapsabet Swamp that were controlled by the local climate. The lower portion of the core (400–225 cm) has an average LSR of 0.08 cm yr^{-1} spanning c. 3023–625 cal yr BP, which increases rapidly in the upper part to an average LSR of 0.44 cm yr^{-1}. Overall, the signals indicate a progressive change from a forested landscape to an open woodland coeval to a decline in terrigenous OM input, suggesting the advent of more wet conditions. This change in western East Africa coincided with the expansion of agriculture and land clearance marking increased human activities and urbanisation in the landscape. We established five separate stages in the depositional history of the Kapsabet Swamp based on the different bulk and molecular proxies. These proxies are mostly well preserved in this swamp because of the depositional conditions (i.e., fast accumulation rate, high TOC content, and acidic environment) and are therefore helpful in understanding the mechanisms driving the regional climate variability on a sub-centennial time scale. These changes have been compared to other studies in East Africa to provide a regional context of the spatiotemporal and climate-environment changes. A summary of the five main stages in the depositional history in Kapsabet Swamp is as follows:

Stage 1 (400 to 310 cm, c. 3023–1670 cal yr BP) records a progression from a cool dryer to a wetter condition. OM was derived from a mix of aquatic plants and humified terrestrial material. MAR was low, and OM preservation declined.

Stage 2 (310 to 265 cm, c. 1670–1187 cal yr BP) is a warm and wet climate with increased productivity and high OM inputs from the catchment and in situ (aquatic) sources. Low MAR continued during this stage, and there was a pronounced variability in the geochemical proxies suggesting a possible influence of the Indian Ocean monsoon system.

Stage 3 (265 to 225 cm, c. 1187–625 cal yr BP) was characterized by gradual warming coeval with the late Holocene Medieval Warm Period. The proxies indicate low productivity and MAR and greater degradation of OM. The dry conditions coincided with the input of increased terrestrial OM rather than aquatic-derived sources.

Stage 4 (225 to 100 cm, c. 625–188 cal yr BP) reflects a cool period with high variability in precipitation and hydrological conditions. The change in sedimentation rate at the beginning of this stage is accompanied by a sharp increase in MAR coinciding with the start of the LIA. The abrupt and sharp increase in the different proxies suggests an inwash of terrestrial-derived OM into a generally dry swamp. As conditions became progressively wetter, there was an increase of aquatic-derived OM. The overall magnitude of variability in different proxies was maximum during this stage, implying highly variable and unstable conditions.

Stage 5 (100 to 0 cm, c. 188 cal yr BP to present) represents a cool and wet climate dominated by aquatic plants but with lower OM preservation and productivity. This period, with muted climatic variability, is similar to the LIA. Additionally, this period coincided with the colonisation of East Africa, which resulted in marked changes in the landscape in terms of soil erosion and deforestation in the catchment.

Changes in the Kapsabet Swamp during the late Holocene were driven by a climate that influenced the deposition of OM, vegetation and peat formation. The climate on the highlands was less variable than in the lowlands, which underwent several periods of drought and intermittent wet conditions accompanied by fluctuations in lake level and other changes. The role of human activities associated with the expansion of agriculture in the catchment mainly prevailed in the lowlands where both natural (lake-level) and human impacts were more evident, the latter, particularly from c. 500 years ago, when the region was settled and colonised. Finally, these valuable isolated peat deposits in highlands face increased challenges today from human incursion and increased destabilisation.

Declaration of Competing Interest

The authors declare there are no conflicting interests.

Acknowledgments

We thank the help extended by Susanne Karlsson and Lena Lundman in the laboratory. Moses Odhiambo and Francis Ogango helped with the fieldwork. Chen Luo helped in making the location map. Constructive suggestions from Robert Patalano and two anonymous reviewers were very helpful in revising the manuscript. The project is supported by Vetensakpsrådet (Grant 348 2013 6760) to JR.

Appendix A. Supplementary data

Supplementary data to this article can be found online at https://doi.org/10.1016/j.palaeo.2021.110475.

References

Achieng', A.O., Raburu, P.O., Okinyi, L., Wanjala, S., 2014. Use of macrophytes in the bioassessment of the health of King'wal Wetland, Lake Victoria Basin, Kenya. Aquat. Ecosyst. Health Manag. 17, 129–136.

Ashley, G.M., Mworia-Maitima, J., Muasya, A.M., Owen, R.B., Driese, S.G., Hover, V.C., Renaut, R.W., Goman, M.F., Mathai, S., Blatt, S.H., 2004. Sedimentation and recent history of a freshwater wetland in a semi-arid environment: Loboi Swamp, Kenya, East Africa. Sedimentology 51, 1–21.

Baker, A., Routh, J., Blaauw, M., Roychoudhury, A.N., 2014. Geochemical records of palaeoenvironmental controls on peat forming processes in the Mfabeni peatland, Kwazulu Natal, South Africa since the late Pleistocene. Palaeogeogr. Palaeoclimatol. Palaeoecol. 395, 95–106. https://doi.org/10.1016/j.palaeo.2013.12.019.

Baker, A., Routh, J., Roychoudhury, A.N., 2016. Biomarker records of palaeoenvironmental variations in subtropical southern Africa since the late Pleistocene: Evidences from a coastal peatland. Palaeogeogr. Palaeoclimatol. Palaeoecol. 451, 1–12. https://doi.org/10.1016/j.palaeo.2016.03.011.

Battistel, D., Argiriadis, E., Kehrwald, N., Spigariol, M., Russell, J.M., Barbante, C., 2017. Fire and human record at Lake Victoria, East Africa, during the early Iron Age: did humans or climate cause massive ecosystem changes? Holocene 27, 997–1007. https://doi.org/10.1177/0959683616678466.

Berke, M.A., Johnson, T.C., Werne, J.P., Grice, K., Schouten, S., Sinninghe Damsté, J.S., 2012. Molecular records of climate variability and vegetation response since the late Pleistocene in the Lake Victoria basin, East Africa. Quat. Sci. Rev. 55, 59–74. https://doi.org/10.1016/j.quascirev.2012.08.014.

Björck, S., Wohlfarth, B., 2002. ^{14}C Chronostratigraphic Techniques in Paleolimnology. In: Last, W.M., Smol, J.P. (Eds.), Tracking Environmental Change Using Lake Sediments, Basin Analysis, Coring, and Chronological Techniques, vol. 1. Kluwer Academic Publishers, Dordrecht, pp. 205–245. https://doi.org/10.1007/0-306-47669-X_10.

Blaauw, M., 2010. Methods and code for 'classical' age-modelling of radiocarbon sequences. Quat. Geochronol. 5, 512–518.

Blaauw, M., Christeny, J.A., 2011. Flexible paleoclimate age-depth models using an autoregressive gamma process. Bayesian Anal. 6, 457–474. https://doi.org/10.1214/11-BA618.

Blaauw, M., van Geel, B., Kristen, I., Plessen, B., Lyaruu, A., Engstrom, D.R., van der Plicht, J., Verschuren, D., 2011. High-resolution ^{14}C dating of a 25,000-year lake-sediment record from equatorial East Africa. Quat. Sci. Rev. 30, 3043–3059. https://doi.org/10.1016/j.quascirev.2011.07.014.

Boivin, N.L., Zeder, M.A., Fuller, D.Q., Crowther, A., Larson, G., Erlandson, J.M., Petraglia, M.D., 2016. Ecological consequences of human niche construction: Examining long-term anthropogenic shaping of global species distributions. Proc. Natl. Acad. Sci. 113, 6388–6396.

Bourbonniere, R.A., Meyers, P.A., 1996. Sedimentary geolipid records of historical changes in the watersheds and productivities of Lakes Ontario and Erie. Limnol. Oceanogr. 41, 352–359. https://doi.org/10.4319/lo.1996.41.2.0352.

Boutton, T., Archer, S.R., Midwood, A.J., Zitzer, S.F., Bol, R., 1998. $\delta^{13}C$ values of soil organic carbon and their use in documenting vegetation change in a subtropical savanna ecosystem. Geoderma 82, 5–41.
Brock, F., Higham, T., Ditchfield, P., Ramsey, C.B., 2010. Current pretreatment methods for AMS radiocarbon dating at the Oxford Radiocarbon Accelerator Unit (ORAU). Radiocarbon 52, 103–112. https://doi.org/10.1017/S0033822200045069.
Bruckner, M., 2006. Climate proxies [WWW Document]. Microb. Life - Educ. Resour. URL. http://serc.carleton.edu/microbelife/topics/proxies/paleoclimate.html (accessed 6.11.17).
Buckles, L.K., Verschuren, D., Weijers, J.W.H., Cocquyt, C., Blaauw, M., Sinninghe Damsté, J.S., 2016. Interannual and (multi-)decadal variability in the sedimentary BIT index of Lake Challa, East Africa, over the past 2200 years: assessment of the precipitation proxy. Clim. Past 12, 1243–1262. https://doi.org/10.5194/cp-12-1243-2016.
Castañeda, I.S., Schouten, S., 2011. A review of molecular organic proxies for examining modern and ancient lacustrine environments. Quat. Sci. Rev. https://doi.org/10.1016/j.quascirev.2011.07.009.
Castañeda, I.S., Werne, J.P., Johnson, T.C., Filley, T.R., 2009. Late Quaternary vegetation history of Southeast Africa: the molecular isotopic record from Lake Malawi. Palaeogeogr. Palaeoclimatol. Palaeoecol. 275, 100–112. https://doi.org/10.1016/j.palaeo.2009.02.008.
Chambers, F.M., Charman, D.J., 2004. Holocene environmental change: contributions from the peatland archive. The Holocene 14, 1–6. https://doi.org/10.1191/0959683604hl684ed.
Chritz, K.L., Cerling, T.E., Freeman, K.H., Hildebrand, E.A., Janzen, A., Prendergast, M. E., 2019. Climate, ecology, and the spread of herding in eastern Africa. Quat. Sci. Rev. 204, 119–132.
Cranwell, P.A., Eglinton, G., Robinson, N., 1987. Lipids of aquatic organisms as potential contributors to lacustrine sediments-II. Org. Geochem. 11, 513–527. https://doi.org/10.1016/0146-6380(87)90007-6.
Czernik, J., Goslar, T., 2001. Preparation of graphite targets in the Gliwice Radiocarbon Laboratory for AMS ^{14}C dating. Radiocarbon 43, 283–291. https://doi.org/10.1017/S0033822200038121.
De Cort, G., Bessems, I., Keppens, E., Mees, F., Cumming, B., Verschuren, D., 2013. Late-Holocene and recent hydroclimatic variability in the Central Kenya Rift Valley: the sediment record of hypersaline lakes Bogoria, Nakuru and Elementeita. Palaeogeogr. Palaeoclimatol. Palaeoecol. 388, 69–80. https://doi.org/10.1016/j.palaeo.2013.07.029.
De Cort, G., Verschuren, D., Ryken, E., Wolff, C., Renaut, R.W., Creutz, M., Van der Meeren, T., Haug, G., Olago, D.O., Mees, F., 2018. Multi-basin depositional framework for moisture-balance reconstruction during the last 1300 years at Lake Bogoria, Central Kenya Rift Valley. Sedimentology 65, 1667–1696. https://doi.org/10.1111/sed.12442.
Driese, S.G., Ashley, G.M., Li, Z.-H., Hover, V.C., Bernhart Owen, R., 2004. Possible late Holocene equatorial palaeoclimate record based upon soils spanning the medieval warm period and Little Ice Age, Loboi Plain, Kenya. Palaeogeogr. Palaeoclimatol. Palaeoecol. 213, 231–250. https://doi.org/10.1016/j.palaeo.2004.07.009.
Edwards, E.J., Osborne, C.P., Strömberg, C.A.E., Smith, S.A., 2010. The origins of C4 grasslands: integrating evolutionary and ecosystem science. Science 328, 587–591.
Ehleringer, J.R., Cerling, T.E., Helliker, B.R., 1997. C4 photosynthesis, atmospheric CO_2, and climate. Oecologia 112, 285–299.
Felton, A.A., Russell, J.M., Cohen, A.S., Baker, M.E., Chesley, J.T., Lezzar, K.E., McGlue, M.M., Pigati, J.S., Quade, J., Curt Stager, J., Tiercelin, J.J., 2007. Paleolimnological evidence for the onset and termination of glacial aridity from Lake Tanganyika, Tropical East Africa. Palaeogeogr. Palaeoclimatol. Palaeoecol. 252, 405–423. https://doi.org/10.1016/j.palaeo.2007.04.003.
Ficken, K.J., Li, B., Swain, D.L., Eglinton, G., 2000. An n-alkane proxy for the sedimentary input of submerged/floating freshwater aquatic macrophytes. Org. Geochem. 31, 745–749. https://doi.org/10.1016/S0146-6380(00)00081-4.
Finkel, R.C., Nishiizumi, K., 1997. Beryllium-10 concentrations in the Greenland Ice Sheet Project 2 ice core from 3-40 ka. J. Geophys. Res. Ocean. 102, 26699–26706. https://doi.org/10.1029/97JC01282.
Galaty, J.G., 1993. Maasai expansion and the new East African pastoralism. Ethnicity Identity East Africa 6, 61–86.
Gillson, L., Waldron, S., Willis, K.J., 2004. Interpretation of soil $\delta^{13}C$ as an indicator of vegetation change in African savannas. J. Veg. Sci. 15, 339–350.
Goslar, T., Czernik, J., Goslar, E., 2004. Low-energy ^{14}C AMS in Poznań Radiocarbon Laboratory, Poland. Nucl. Inst. Methods Phys. Res. B 223, 5–11. https://doi.org/10.1016/j.nimb.2004.04.005.
Grzybowski, M., Glińska-Lewczuk, K., 2020. The principal threats to the peatlands habitats, in the continental bioregion of Central Europe – a case study of peatland conservation in Poland. J. Nat. Conserv. 53, 125778. https://doi.org/10.1016/j.jnc.2019.125778.
Halfman, J.D., Johnson, T.C., Finney, B.P., 1994. New AMS dates, stratigraphic correlations and decadal climatic cycles for the past 4 ka at Lake Turkana, Kenya. Palaeogeogr. Palaeoclimatol. Palaeoecol. 111, 83–98. https://doi.org/10.1016/0031-0182(94)90349-2.
Hamilton, A.C., 1982. Environmental History of East Africa: A Study of the Quaternary. Academic Press, London, p. 328.
Hamilton, A., Taylor, D., Vogel, J., 1986. Early forest clearance and environmental degradation in south-West Uganda. Nature 320, 164–167.
Högberg, P., 1997. Tansley Review no. 95 ^{15}N natural abundance in soil-plant systems. New Phytol. 137, 179–203. https://doi.org/10.1046/j.1469-8137.1997.00808.x.
Jennings, D.J., 1964. Geology of the Kapsabet-Plateau area: degree sheet 34, SW quarter (with coloured geological map). Geol. Survey Kenya. 63, 43.
Jha, D.K., Sanyal, P., Philippe, A., 2020. Multi-proxy evidence of late Quaternary climate and vegetational history of north-Central India: Implication for the Paleolithic to Neolithic phases. Quat. Sci. Rev. 229, 106121.
Johnson, T.C., Halfman, J.D., Showers, W.J., 1991. Paleoclimate of the past 4000 years at Lake Turkana, Kenya, based on the isotopic composition of authigenic calcite. Palaeogeogr. Palaeoclimatol. Palaeoecol. 85, 189–198. https://doi.org/10.1016/0031-0182(91)90158-N.
Keddy, P.A., 2010. Wetland Ecology: Principles and Conservation. Cambridge University Press, p. 497.
Kiage, L.M., Liu, K., 2006. Late Quaternary paleoenvironmental changes in East Africa: a review of multiproxy evidence from palynology, lake sediments, and associated records. Prog. Phys. Geogr. Earth Environ. 30, 633–658. https://doi.org/10.1177/0309133306071146.
Konecky, B., Russell, J., Huang, Y., Vuille, M., Cohen, L., Street-Perrott, F.A., 2014. Impact of monsoons, temperature, and CO_2 on the rainfall and ecosystems of Mt. Kenya during the Common Era. Palaeogeogr. Palaeoclimatol. Palaeoecol. 396, 17–25. https://doi.org/10.1016/j.palaeo.2013.12.037.
Levin, N.E., 2015. Environment and climate of early human evolution. Annu. Rev. Earth Planet. Sci. 43, 405–429.
Marchant, R., Richer, S., Capitani, C., Courtney-Mustaphi, C., Prendergast, M., Stump, D., Boles, O., Lane, P., Wynne-Jones, S., Vázquez, C.F., Wright, D., Boivin, N., Lang, C., Kay, A., Phelps, L., Fuller, D., Widgren, M., Punwong, P., Lejju, J., Gaillard-Lemdahl, M.-J., Morrison, K.D., Kaplan, J., Benard, J., Crowther, A., Cuní-Sanchez, A., de Cort, G., Deere, N., Ekblom, A., Farmer, J., Finch, J., Gillson, L., Githumbi, E., Kabora, T., Kariuki, R., Kinyanjui, R., Kyazike, E., Muiruri, V., Mumbi, C., Muthoni, R., Muzuka, A., Ndiema, E., Nzaba, C., Olago, D., Onjala, I., Schrijver, A.P., Petek, N., Platts, P.J., Rucina, S., Shoemaker, A., Thornton-Barnett, S., van der Plas, G., Watson, L., Williamson, D., 2018. Drivers and trajectories of land cover change in East Africa: Human and environmental interactions from 6000 years ago to present. Earth-Sci. Rev. 178, 322–378. https://doi.org/10.1016/j.earscirev.2017.12.010.
Martinelli, L.A., Piccolo, M.C., Townsend, A.R., Vitousek, P.M., Cuevas, E., McDowell, W., Robertson, G.P., Santos, O.C., Treseder, K., 1999. Nitrogen stable isotopic composition of leaves and soil: Tropical versus temperate forests. Biogeochemistry 46, 45–65. https://doi.org/10.1007/BF01007573.
Maua, J.O., Mugatsia Tsingalia, H., Cheboiwo, J., Odee, D., 2020. Population structure and regeneration status of woody species in a remnant tropical forest: a case study of south Nandi forest, Kenya. Global Ecol. Conserv. 21, e00820.
Mayewski, P.A., Rohling, E., Curtstager, J., Karlén, W., Maasch, K., Davidmeeker, L., Meyerson, E., Gasse, F., Vankreveld, S., Holmgren, K., 2004. Holocene climate variability. Quat. Res. 62, 243–255. https://doi.org/10.1016/j.yqres.2004.07.001.
McKinney, D.E., Carson, D.M., Clifford, D.J., Minard, R.D., Hatcher, P.G., 1995. Off-line thermochemolysis versus flash pyrolysis for the in situ methylation of lignin: is pyrolysis necessary? J. Anal. Appl. Pyrolysis 34, 41–46. https://doi.org/10.1016/0165-2370(94)00865-X.
Meyers, P.A., 1994. Preservation of elemental and isotopic source identification of sedimentary organic matter. Chem. Geol. 114, 289–302. https://doi.org/10.1016/0009-2541(94)90059-0.
Meyers, P., 2003. Applications of organic geochemistry to paleolimnological reconstructions: a summary of examples from the Laurentian Great Lakes. Organic Geochemistry 34, 261–289.
Meyers, P.A., Ishiwatari, R., 1995. Organic Matter Accumulation Records in Lake Sediments. In: Lerman, A., Imboden, D., Gat, J.R. (Eds.), Physics and Chemistry of Lakes. Springer, Berlin Heidelberg, pp. 279–328. https://doi.org/10.1007/978-3-642-85132-2_10.
Meyers, P.A., Teranes, J.L., 2002. Sediment organic matter. In: Last, W.M., Smol, J.P. (Eds.), Tracking Environmental Change Using Lake Sediments. Kluwer Academic Publishers, Dordrecht, pp. 239–269. https://doi.org/10.1007/0-306-.
Momanyi, S., Ariya, G., 2015. Sustainable wetland resource utilization through eco-tourism development for poverty reduction: a case study of Kingwal swamp, Kenya. Eur. J. Business Soc. Sci. 4, 56-73.47670-3_9.
Msaky, E.S., Livingstone, D., Davis, O.K., 2005. Paleolimnological investigations of anthropogenic environmental change in Lake Tanganyika. V. Palynological evidence for deforestation and increased erosion. J. Paleolimnol. 34, 73–83.
Muzuka, A.N.N., 1999. Isotopic compositions of tropical East African flora and their potential as source indicators of organic matter in coastal marine sediments. J. Afr. Earth Sci. 28, 757–766.
Nakintu, J., Lejju, J.B., 2016. A 10000 ^{14}C yr diatom record from Napoleon Gulf and Sango Bay, Lake Victoria. Quat. Int. 404, 180–181. https://doi.org/10.1016/j.quaint.2015.08.114.
Niang, I., Ruppel, O., Abdrabo, M., Essel, A., Lennard, C., 2014. Africa, Climate Change 2014: Impacts, Adaptation and Vulnerability—Contributions of the Working Group II to the Fifth Assessment Report of the Intergovernmental Panel on Climate Change. Cambridge University Press, NY, USA.
Nicholson, S., 2000. Land surface processes and Sahel climate. Rev. Geophys. 38, 117–139. https://doi.org/10.1029/1999RG900014.
Olago, D.O., Street-Perrott, F.A., Perrott, R.A., Ivanovich, M., Harkness, D.D., Odada, E. O., 2000. Long-term temporal characteristics of palaeomonsoon dynamics in equatorial Africa. Glob. Planet. Chang. 26, 159–171. https://doi.org/10.1016/S0921-8181(00)00041-2.
Olago, D., Opere, A., Barongo, J., 2009. Holocene palaeohydrology, groundwater and climate change in the lake basins of the Central Kenya Rift. Hydrol. Sci. J. 54, 765–780. https://doi.org/10.1623/hysj.54.4.765.
Olaka, L.A., Odada, E.O., Trauth, M.H., Olago, D.O., 2010. The sensitivity of East African rift lakes to climate fluctuations. J. Paleolimnol. 44, 629–644. https://doi.org/10.1007/s10933-010-9442-4.

Opiyo, B., Gebregiorgis, D., Cheruiyot, V.C., Deocampo, D.M., Kiage, L.M., 2019. Late Quaternary paleoenvironmental changes in tropical eastern Africa revealed by multi–proxy records from the Cherangani Hills, Kenya. Quat. Sci. Rev. 222, 105907. https://doi.org/10.1016/j.quascirev.2019.105907.

Parish, F., Sirin, A., Charman, D., Joosten, H., Minaeva, T., 2008. Assessment on Peatlands, Biodiversity and Climate Change. Main Report. Global Environment Centre, Kuala Lumpur and Wetlands International, Wageningen.

Payne, R.J., Malysheva, E., Tsyganov, A., Pampura, T., Novenko, E., Volkova, E., Babeshko, K., Mazei, Y., 2015. A multi-proxy record of Holocene environmental change, peatland development and carbon accumulation from Staroselsky Moch peatland, Russia. The Holocene 26, 1–13. https://doi.org/10.1177/0959683615608692.

Peters, K.E., Walters, C.C., Moldowan, J.M., 2005. The Biomarker Guide. In: Biomarkers and Isotopes in the Petroleum Exploration and Earth History, , 2nd editionVol. 2. Cambridge University Press. https://doi.org/10.1073/pnas.0703993104.

Posa, M.R.C., Wijedasa, L.S., Corlett, R.T., 2011. Biodiversity and conservation of tropical peat swamp forests. Bioscience 61, 49–57. https://doi.org/10.1525/bio.2011.61.1.10.

Raburu, P., 2005. National Lessons Learnt Consultancy on Wetlands Component Activities.

Reimer, P.J., Baillie, M.G.L., Bard, E., Warren Beck, J., Blackwell, P.G., Buck, C.E., Burr, G.S., Lawrence Edwards, R., Friedrich, M., Guilderson, T.P., Hogg, A.G., Hughen, K.A., Kromer, B., McCormac, G., Manning, Sturt, Reimer, R.W., Southon, J. R., Stuiver, M., van der Plicht, J., Weyhenmeyer, C.E., Manning, S., Weyhenmeyer, C., Reimer, P.J., Baillie, M.G.L., Reimer, R.W., Blackwell, P.G., Buck, C.E., Burr, G.S., Guilderson, T.P., Hogg, A.G., Hughen, K.A., Southon, J.R., Weyhenmeyer, C.E., 2006. Radiocarbon calibration curve spanning 0 to 50,000 years BP based on paired Th-230/U-234/U-238 and C-14 dates on pristine corals by R.G. Fairbanks et al. (Quaternary Science Reviews 24 (2005) 1781–1796) and Extending the radiocarbon calibration beyond 26,000 years before present using fossil corals by T.-C. Chin et al. (Quaternary Science Reviews 24 (2005) 1797–1808). Quat. Sci. Rev. 25, 855–862. https://doi.org/10.1016/j.quascirev.2005.09.009.

Robinson, D., 2001. $\delta^{15}N$ as an integrator of the nitrogen cycle. Trends Ecol. Evol. 16, 153–162.

Routh, J., Hugelius, G., Kuhry, P., Filley, T., Tillman, P.K., Becher, M., Crill, P., 2014. Multi-proxy study of soil organic matter dynamics in permafrost peat deposits reveal vulnerability to climate change in the European Russian Arctic. Chem. Geol. 368, 104–117. https://doi.org/10.1016/j.chemgeo.2013.12.022.

Russell, J.M., Johnson, T.C., 2005. Late Holocene climate change in the North Atlantic and equatorial Africa: Millennial-scale ITCZ migration. Geophys. Res. Lett. 32, L17705 https://doi.org/10.1029/2005GL023295.

Russell, J.M., Johnson, T.C., 2007. Little Ice Age drought in equatorial Africa: Intertropical Convergence Zone migrations and El Niño–Southern Oscillation variability. Geology 35, 21. https://doi.org/10.1130/G23125A.1.

Russell, J.M., Verschuren, D., Eggermont, H., 2007. Spatial complexity of "Little Ice Age" climate in East Africa: Sedimentary records from two crater lake basins in western Uganda. Holocene 17, 183–193. https://doi.org/10.1177/0959683607075832.

Ryves, D.B., Clarke, A.L., Appleby, P.G., Amsinck, S.L., Jeppesen, E., Landkildehus, F., Anderson, N.J., 2004. Reconstructing the salinity and environment of the Limfjord and Vejlerne Nature Reserve, Denmark, using a diatom model for brackish lakes and fjords. Can. J. Fish. Aquat. Sci. 61, 1988–2006. https://doi.org/10.1139/f04-127.

Ryves, D.B., Mills, K., Bennike, O., Brodersen, K.P., Lamb, A.L., Leng, M.J., Russell, J.M., Ssemmanda, I., 2011. Environmental change over the last millennium recorded in two contrasting crater lakes in western Uganda, eastern Africa (Lakes Kasenda and Wandakara). Quat. Sci. Rev. 30, 555–569. https://doi.org/10.1016/j.quascirev.2010.11.011.

Schefuß, E., Schouten, S., Jansen, J.H.F., Sinnighe Damsté, J.S., 2003. African vegetation controlled by tropical sea surface temperatures in the mid-Pleistocene period. Nature 422, 418–421.

Sitienei, J.A., Jiwen, G., Mupenzi, P.J., 2012. Impacts of anthropogenic activities and climate change on wetland ecology: Case of Sitatunga, *Tragelaphus spkeii* at Kingwal Wetland, Kenya. East Africa J. Sci. Tech. 1, 1–8.

Songok, C.K., Kipkorir, E.C., Mugalavai, E.M., 2011. Integration of indigenous knowledge systems into climate change adaptation and enhancing food security in Nandi and Keiyo districts, Kenya. Exp. Clim. Change Adapt. Africa 69–95. https://doi.org/10.1007/978-3-642-22315-0_5.

Ssemmanda, I., Vincens, A., 2002. Vegetation Changes and their Climatic Implications for the Lake Victoria Region during the Late Holocene. Springer, Dordrecht, pp. 509–523. https://doi.org/10.1007/0-306-48201-0_21.

Ssemmanda, I., Ryves, D.B., Bennike, O., Appleby, P.G., 2005. Vegetation history in western Uganda during the last 1200 years: a sediment-based reconstruction from two crater lakes. Holocene 15, 119–132. https://doi.org/10.1191/0959683605hl774rp.

Ssemmanda, I., Gelorini, V., Verschuren, D., 2014. Sensitivity of East African savannah vegetation to historical moisture-balance variation. Clim. Past 10, 2067–2080. https://doi.org/10.5194/cp-10-2067-2014.

Stager, J.C., Johnson, T.C., 2000. A 12,400 ^{14}C yr offshore diatom record from east-Central Lake Victoria, East Africa. J. Paleolimnol. 23, 373–383. https://doi.org/10.1023/A:1008133727763.

Stager, J.C., Johnson, T.C., 2007. The Late Pleistocene desiccation of Lake Victoria and the origin of its endemic biota. Hydrobiologia 596, 5–16.

Stager, J.C., Ryves, D., Cumming, B.F., David Meeker, L., Beer, J., 2005. Solar variability and the levels of Lake Victoria, East Africa, during the last millennium. J. Paleolimnol. 33, 243–251. https://doi.org/10.1007/s10933-004-4227-2.

Strack, M., 2008. Peatlands and Climate Change. The University of Calgary, Canada. Ph. D. Thesis.

Stuiver, M., Polach, H.A., 1977. Discussion reporting of ^{14}C data. Radiocarbon 19, 355–363. https://doi.org/10.1017/S0033822200003672.

Stuiver, M., Reimer, P.J., Braziunas, T.F., 1998. High-precision radiocarbon age calibration for terrestrial and marine samples. Radiocarbon 40, 1127–1151. https://doi.org/10.1017/S0033822200019172.

Talbot, M.R., Lærdal, T., 2000. The late Pleistocene - Holocene palaeolimnology of Lake Victoria, East Africa, based upon elemental and isotopic analyses of sedimentary organic matter. J. Paleolimnol. 23, 141–164. https://doi.org/10.1023/A:1008029400463.

Taylor, D.M., 1990. Late Quaternary pollen records from two Ugandan mires: evidence for environmental change in the Rukiga highlands of Southwest Uganda. Palaeogeogr., Palaeoclimat. Palaeecol 80, 283–300.

Tiercelin, J.-J., Lezzar, K.-E., 2002. A 300 million years history of Rift Lakes in Central and East Africa: An updated broad review. In: Odada, E.O., Olago, D.O. (Eds.), The East African Great Lakes: Limnology, Palaeolimnology and Biodiversity. Kluwer Academic Publishers, Dordrecht. https://doi.org/10.1007/0-306-48201-0_1.

Tierney, J.E., Smerdon, J.E., Anchukaitis, K.J., Seager, R., 2013. Multidecadal variability in East African hydroclimate controlled by the Indian Ocean. Nature 493, 389–392. https://doi.org/10.1038/nature11785.

Tiunov, A.V., 2007. Stable isotopes of carbon and nitrogen in soil ecological studies. Biol. Bull. 34, 395–407. https://doi.org/10.1134/S1062359007040127.

Trauth, M.H., Maslin, M.A., Deino, A.L., Junginger, A., Lesoloyia, M., Odada, E.O., Olago, D.O., Olaka, L.A., Strecker, M.R., Tiedemann, R., 2010. Human evolution in a variable environment: the amplifier lakes of Eastern Africa. Quat. Sci. Rev. 29, 2981–2988. https://doi.org/10.1016/j.quascirev.2010.07.007.

Verschuren, D., 2001. Reconstructing fluctuations of a shallow East African lake during the past 1800 yrs from sediment stratigraphy in a submerged crater basin. J. Paleolimnol. 25, 297–311. https://doi.org/10.1023/A:1011150300252.

Verschuren, D., 2004. Decadal and century-scale climate variability in tropical Africa during the past 2000 years. In: Battarbee, R.W., Gasse, F., Stickley, C.E. (Eds.), Past Climate Variability through Europe and Africa. Springer Netherlands, Dordrecht, pp. 139–158. https://doi.org/10.1007/978-1-4020-2121-3_8.

Verschuren, D., Russell, J.M., 2009. Paleolimnology of African lakes: beyond the exploration phase. PAGES News 17, 112–114. Doi:10.22498/pages.17.3.112.

Verschuren, D., Laird, K.R., Cumming, B.F., 2000. Rainfall and drought in equatorial East Africa during the past 1,100 years. Nature 403, 410–414. https://doi.org/10.1038/35000179.

Verschuren, D., Johnson, T.C., Kling, H.J., Edgington, D.N., Leavitt, P.R., Brown, E.T., Talbot, M.R., Hecky, R.E., 2002. History and timing of human impact on Lake Victoria. East Africa. Proc. Royal Soc. London. Ser. B Biol. Sci. 269, 289–294. https://doi.org/10.1098/rspb.2001.1850.

Verschuren, D., Sinninghe Damsté, J.S., Moernaut, J., Kristen, I., Blaauw, M., Fagot, M., Haug, G.H., 2009. Half-precessional dynamics of monsoon rainfall near the East African Equator. Nature 462, 637–641. https://doi.org/10.1038/nature08520.

Vincens, A., 1989. Paleoenvironnements du bassin Nord-Tanganyika (Zaire, Burundi, Tanzanie) au cours des 13 derniers mille ans: apport de la palynologie. Review of Palaeobotany and Palynology 61, 69–88.

Wakeham, S.G., Peterson, M.L., Hedges, J.I., Lee, C., 2002. Lipid biomarker fluxes in the Arabian Sea, with a comparison to the equatorial Pacific Ocean. Deep. Res. Part II Top. Stud. Oceanogr. 49, 2265–2301. https://doi.org/10.1016/S0967-0645(02)00037-1.

WoldeGabriel, G., Olago, D., Dindi, E., Owor, M., 2016. Genesis of the East African Rift System. In: Schager, M. (Ed.), Soda Lakes of East Africa. Springer International Publishing, pp. 25–59. https://doi.org/10.1007/978-3-319-28622-8_2.

Zech, M., 2006. The Use of biomarker and stable isotope analyses in palaeopedology. In: Reconstruction of Middle and Late Quaternary environmental and Climate History, with EXAMPLES from Mt. Kilimanjaro, NE Siberia and NE Argentina. Ph.D. Thesis. Bayreuth University, Germany.

Zheng, Y., Zhou, W., Meyers, P.A., Xie, S., 2007. Lipid biomarkers in the Zoigê-Hongyuan peat deposit: Indicators of Holocene climate changes in West China. Org. Geochem. 38, 1927–1940. https://doi.org/10.1016/j.orggeochem.2007.06.012.